



ELSEVIER

Contents lists available at SciVerse ScienceDirect

## Journal of Solid State Chemistry

journal homepage: [www.elsevier.com/locate/jssc](http://www.elsevier.com/locate/jssc)

# Mild hydrothermal synthesis, crystal structure, photoluminescence properties and emission quantum yield of a new zirconium germanate with garnet-type structure

Stanislav Ferdov<sup>a,\*</sup>, Rute A.S. Ferreira<sup>b</sup>, Zhi Lin<sup>c</sup>, Zhengying Wu<sup>c</sup><sup>a</sup> Department of Physics, University of Minho, 4800-058 Guimarães, Portugal<sup>b</sup> Department of Physics, CICECO, University of Aveiro, 3810-193 Aveiro, Portugal<sup>c</sup> Department of Chemistry, CICECO, University of Aveiro, 3810-193 Aveiro, Portugal

## ARTICLE INFO

## Article history:

Received 9 January 2012

Received in revised form

30 January 2012

Accepted 31 January 2012

Available online 7 February 2012

## Keywords:

Hydrothermal synthesis

Garnet

Zirconium germanate

Crystal structure

Photoluminescence

## ABSTRACT

The mild hydrothermal synthesis, crystal structure, photoluminescence properties and emission quantum yield of a new sodium zirconium germanate are reported. This material and the method for its preparation represent for the first time a germanium garnet-type material synthesized at autogenous pressure and temperature at 230 °C. The crystal structure was determined by starting from the crystallographic parameters of a common garnet structure and it represents not only a new chemical combination of atoms but also combination of oxidation states in garnet structure. The framework consists of interconnected corner sharing  $\text{GeO}_4$  tetrahedra and  $\text{ZrO}_6$  octahedra which form small cavities that accommodate charge compensation  $\text{Na}^+$  cations. In the course of synthesis the structure can be functionalized by *in situ* doping with different percentage of  $\text{Eu}^{3+}$  ions. This structural flexibility is used to explore the photoluminescent behavior of the active centers embedded in garnet-type host. The materials display the  $\text{Eu}^{3+} \ ^5\text{D}_0 \rightarrow \ ^7\text{F}_{0-4}$  transitions under excitation via intra- $^4\text{f}_6$  excitation levels and through the  $\text{O}^{2-} \rightarrow \text{Eu}^{3+}$  ligand-to-metal charge transfer. A maximum  $^5\text{D}_0$  quantum efficiency and emission quantum yield values (ca. 0.28 and  $0.04 \pm 0.01$ , respectively) were found for the low  $\text{Eu}^{3+}$ -containing sample, suggesting the presence of concentration quenching effects at higher  $\text{Eu}^{3+}$ -content (5%).

© 2012 Elsevier Inc. All rights reserved.

## 1. Introduction

The garnet group includes a large family of orthosilicate minerals with the general formula  $\text{A}_3\text{B}_2(\text{SiO}_4)_3$  ( $\text{A}^{\text{II}} = \text{Ca, Mg, Fe}$  and  $\text{B}^{\text{III}} = \text{Al, Cr, Fe}$ ), in which A and B cations are 8- and 6-coordinated by oxygen, respectively. Since this structure consists of 8-, 6-, and 4-coordinated cation sites, a large variety of cations in different valence states, for example, alkali, alkaline earth, rare-earth, and transition metal ions, can be introduced into garnet structure by replacing either A or B or Si sites [1]. This flexibility makes garnets useful in different areas. For instance, garnets containing transition and rare-earth elements are applied as magnetic [2] and luminescent materials [3], advanced ceramics [4], oxygen ion conductors [5], batteries [6], and materials for solid state lasers [7–11]. Among the members of the garnet group yttrium aluminum (YAG) and yttrium gallium (YGG) have important optical applications after they are doped with rare-earth elements [12]. The rare-earth doped garnets attract considerable

attention as host crystals for near-infrared solid state lasers as well as for optoelectronics devices, including computer memories, microwave optical elements and as laser active media with applications in medical surgery, optical communications and coherent laser radar [13–15].

In majority of the experiments, the synthetic garnets are prepared at high temperatures via solid-state reaction and the mild hydrothermal syntheses are applied successfully only for a few members of the group which can be achieved at temperatures below 180 °C [16]. Concerning the preparation of germanium zirconate garnet-type materials we found only one report describing a high temperature (1400 °C) synthesis of  $\text{Ca}_4\text{ZrGe}_3\text{O}_{12}$  [17].

In this respect, it is a challenge to find a fast and cheap low temperature method for preparation of new members of the garnet family. In the work here we present one step low temperature, autogenous pressure hydrothermal synthesis of a new sodium germanium zirconium garnet-type material. The described method for preparation can profit from the structural flexibility and it is efficient for *in situ* doping with rare-earth ( $\text{Eu}^{3+}$ ) element. This way of optical functionalization is explored by photoluminescent study of the doped material.

\* Corresponding author. Fax: +351 253 510 461.

E-mail address: [sferdov@fisica.uminho.pt](mailto:sferdov@fisica.uminho.pt) (S. Ferdov).

## 2. Experimental

In a typical synthesis of  $\text{Na}_3\text{Zr}_{1.8}\text{Ge}_3\text{O}_{10}(\text{OH})_{2.2}$ , a solution of 0.79 g of sodium hydroxide (Aldrich) in 9.64 g of distilled water was mixed with 0.51 g  $\text{GeO}_2$  (Aldrich) and 0.1 g of zirconium(IV) chloride (Aldrich) hydrolyzed in 6.91 g of water. The resulting mixture was homogenized for 40 min and then transferred into a Teflon-lined autoclave (45 mL). The crystallization was performed under static conditions at 230 °C for 6 day. After fast cooling with flowing water the run product was filtered with distilled water and dried at 40 °C for one day. The phase crystallizes as sub-micron (200–700 nm) ball-shaped particles (Fig. 1). The doping with  $\text{Eu}^{3+}$  was performed as follows 1 (G30) or 5 (G27) mole percent of Zr source was replaced by europium(III) chloride ( $\text{EuCl}_3 \cdot 6\text{H}_2\text{O}$ ) and the crystallization was performed under static conditions at 230 °C for 15 day and 240 °C for 9 day, respectively.

The scanning electron microscopy (SEM) images and chemical analysis (EDS) were carried out using a scanning electron microscope Hitachi S-4100 equipped with a Römteck EDS System. X-ray diffraction data were collected in a flat-plate geometry in  $\theta$ - $2\theta$  step-scan mode in the angle interval 10°–140° ( $2\theta$ ), at steps of 0.02° ( $2\theta$ ) and counting time of 2863 s/step on a Bruker D8 Discover diffractometer, equipped with Cu tube and parallel Lynx Eye detector. Fourier transformed infrared (FT-IR) spectrum of powdered sample suspended in KBr pellets was collected in the range of 400–4000  $\text{cm}^{-1}$  using a Mattson 7000 spectrometer, with resolution 2  $\text{cm}^{-1}$ . Thermogravimetry (TG) curve was collected with a Shimadzu TG-50 analyzer. The sample was heated in air with a rate of 5 °C/min.

The photoluminescence spectra were recorded at room temperature on a Fluorolog-3 Model FL3-2T with double excitation spectrometer and a single emission spectrometer (TRIAx 320) coupled to a R928 Hamamatsu photomultiplier, using a front face acquisition mode. The excitation source was a 450 W Xenon lamp. Emission was corrected for the spectral response of the spectrofluorimeter and the excitation spectra were weighed for the spectral distribution of the lamp intensity using a photodiode reference detector. The decay curves were acquired at low temperature with the setup described for the luminescence spectra using a pulsed Xe–Hg lamp (6  $\mu\text{s}$  pulse at half width and 20–30  $\mu\text{s}$  tail). The absolute emission quantum yields were measured at room temperature using a quantum yield

measurement system C9920-02 from Hamamatsu with a 150 W Xenon lamp coupled to a monochromator for wavelength discrimination, an integrating sphere as sample chamber and a multi channel analyzer for signal detection. Three measurements were made for each sample so that the average value is reported. The method is accurate to within 10%.

## 3. Results and discussion

### 3.1. Infrared (FTIR) spectroscopy

The FTIR spectrum exhibits bands at 3430, 2924, 2847, 1630, 761, and 436  $\text{cm}^{-1}$  (Fig. 2). The broadband between 3000 and 3650  $\text{cm}^{-1}$  arises from the O–H bond stretching modes and demonstrates a presence of hydrous species. The bands at 3430 and 1630  $\text{cm}^{-1}$  (HO–H bond bending) indicate the presence of surface water molecules [18]. Generally the band corresponding to the O–H stretching mode appears as a narrow peak [18], however in the spectrum of Fig. 2 it appears as a part of shoulder probably due to the abundance of hydrous species on the surface and its partial occupation. Upon heating the release of the OH groups explains the weight loss detected by TG. The weak stretching bands at 2924 and 2847  $\text{cm}^{-1}$  result from a small amount of Si–H [19] species due to the preparation of the FTIR pellet in an agate mortar. The intense band at 760  $\text{cm}^{-1}$  is most likely due to the vibrations of Ge–O [20]. The bands appearing at 436  $\text{cm}^{-1}$  may be due to the vibrations of the Zr–O bending mode [21, 22].

### 3.2. TG

Thermogravimetry curve (Fig. 3) shows a weight loss of around 7%. The presence of 2.2 OH groups from structure refinement results in 5.8 wt% mass loss. The rest should be due to surface attached hydrous species since the sample consists of small particles with high surface area.

### 3.3. Crystal structure

The powder X-ray diffraction pattern of  $\text{Na}_3\text{Zr}_{1.8}\text{Ge}_3\text{O}_{10}(\text{OH})_{2.2}$  was indexed by using the DICVOL program [23] and a cubic cell was obtained,  $a = 12.709(6)$  Å. These data were used for search in the available structural databases (ICDD – International Center for Diffraction Data and ICSD – Inorganic Crystal Structure Database) which indicated a similarity between the present phase and common garnet structure. Additionally, a careful inspection of

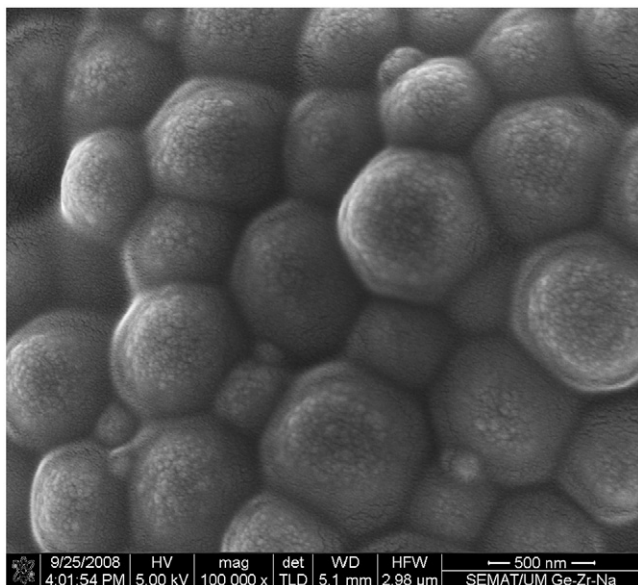


Fig. 1. SEM image of the as-synthesized  $\text{Na}_3\text{Zr}_{1.8}\text{Ge}_3\text{O}_{10}(\text{OH})_{2.2}$ .

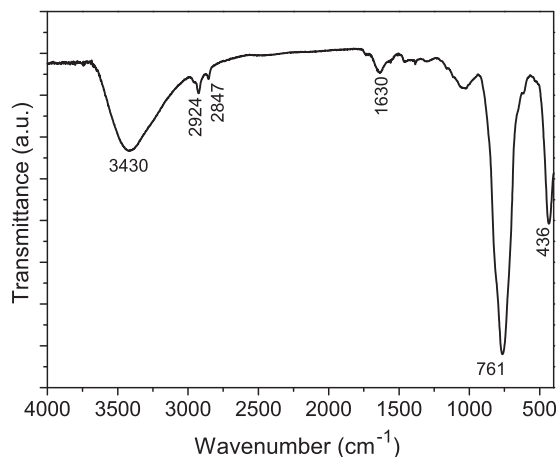


Fig. 2. FTIR spectrum of the as-synthesized  $\text{Na}_3\text{Zr}_{1.8}\text{Ge}_3\text{O}_{10}(\text{OH})_{2.2}$ .

Download English Version:

<https://daneshyari.com/en/article/7761092>

Download Persian Version:

<https://daneshyari.com/article/7761092>

[Daneshyari.com](https://daneshyari.com)